LE STUDIUM
Loire Valley
Institute for Advanced Studies

LE STUDIUM Multidisciplinary Journal
ISSN 2669-7807
www.lestudium-ias.com

FELLOWSHIP FINAL REPORT

Microphysical and optical characterization of aerosols in urban areas by in situ and balloon flight measurements: application to the study of air quality in Burkina Faso, West Africa.

Nébon Bado[1,2], Berthet Gwenaël[1], Valery Catoire[1]

[1]Laboratory of Physics and Chemistry of the Environment and Space (LPC2E), CNRS, Orléans
[2]Renewable Thermal Energy Laboratory, Joseph KI-ZERBO University, Ouagadougou, Burkina Faso

REPORT INFO
Fellow: **Dr Nébon BADO**
From Joseph KI-ZERBO University, Burkina Faso
Host laboratory in region Centre-Val de Loire: Laboratory of Physics and Chemistry of the Environment and Space (LPC2E), CNRS, Orléans
Host scientist: **Dr Gwenaël Berthet**
Period of residence in region Centre-Val de Loire: Sep 2025 - Nov 2025

Keywords:
Aerosol, Characterization, Optical instruments, Global model, Burkina Faso

ABSTRACT

The work presented is a report on a research stay as part of LE STUDIUM for visiting researchers from September 1 to November 30, 2025, at the Laboratory of Physics and Chemistry of the Environment and Space (LPC2E) of the CNRS in Orléans. This is a research stay whose objective is to apply an in-depth methodology for the microphysical, optical, and radiative characterization of aerosols at the surface and at altitude. This technique is based on in situ measurements taken by the LOAC instrument during flights using weather balloons, climate model simulations, and data from airborne and satellite sensors. This enabled us to understand the measurement methodology using the LOAC instrument, which has already been tested by the CNRS's LPC2E, and aerosol modeling using ECSM2 model simulations. Based on the measurement campaigns carried out, we analyzed the aerosol profile as well as that of PM1, PM2.5, and PM10, and the volume size distribution of the particles. Also, based on aerosol extinction evaluated using the Mie code, we were able to determine the aerosol optical depth (AOD), which is an integration of the extinction coefficient across the atmospheric layer. In addition, this trip was an opportunity to participate in a validation study of the ATLID lidar aboard the EarthCare satellite, which has been in orbit since May 2024. This has enabled us to learn a new approach to the optical and microphysical characterization of aerosols that can be applied in Burkina Faso and West Africa in general.

1- Introduction

Desert aerosols are mineral particles that are often aggregated, complex in shape, and cover a very wide range of sizes from around 100 nanometers to several tens of micrometers [1]. Burkina Faso, a sub-Saharan African country, is highly exposed to Saharan dust due to long-distance transport in the air, in addition to anthropogenic emissions linked to road traffic, as most of its roads are unpaved, which promotes the local resuspension of dust [2]. Added to this is the poor management of household waste, which releases biogenic debris after decomposition. Furthermore, this waste is very often burned in the open air, which causes carbon particle emissions, in addition to the numerous bush fires in rural areas during winter and spring following the development of agricultural land [3], [4], [5]. All these actions contribute significantly to the production of combustion particles, which add to mineral dust, creating an aerosol plume with a very complex climate, environmental, and health impact that is difficult to quantify precisely [5], [6]. These aerosols have multiple effects on the climate by extinguishing solar radiation and modifying cloud properties [7]. They also influence the geochemical cycle and the fertility of oceans and soils through erosion and deposition, and affect health by irritating the respiratory tract [1], [8]. Several studies conducted at the national level have enabled the optical, microphysical, and radiative characterization of aerosols based on in situ measurements, satellite observations, and climate model reanalyses [9], [10], [11]. However, this work remains incomplete due to the high variability of the aerosol population, defined by the chemical composition and size of particles linked to numerous emission sources and strong population growth [3], [12]. In addition, the lack of ground-based measuring instruments such as solar photometers, lidar, and aerosol counters in Burkina Faso in particular is a major limitation to any study aimed at establishing a permanent database. However, it is important to understand and quantify the aerosol cycle as accurately as possible in order to model processes and predict expected changes in the context of climate change. It is in this context that our work is situated, with the objective of applying a comprehensive methodology for the microphysical, optical, and radiative characterization of aerosols in Burkina Faso, both at the surface and at altitude, based on in situ measurements using optical instrumentation combined with chemistry–climate simulations, for the study of air quality and the climatic impact of aerosols, covering all seasons affected by different emission sources. The methodology, which has been tested at LPC2E/CNRS in Orléans and is particularly lacking in Burkina Faso, will be a first in this region of Africa, with a strategy that will be multi-year in nature through long-term inter-institutional collaboration.

2- Experimental details

2.1. LOAC Instrument

2.1.1. Presentation of LOAC

LOAC (Light Optical Aerosol Counter) is a miniaturized aerosol counter developed between 2010 and 2013 as part of a project by the French National Research Agency. This project is a collaboration between public and private partners, including the Laboratory of Environmental and Space Physics and Chemistry (LPC2E, CNRS/ University of Orleans), the Laboratory of Climate and

Environmental Sciences (LSCE, CNRS / CEA), the Aerology Laboratory (LA, CNRS / University of Toulouse), the companies Environnement-SA and Aérophile, and with logistical support from the National Center for Space Studies (CNES). One of the motivations for this development was participation in the international ChArMEx campaign dedicated to studying the Mediterranean basin in the summer of 2013. The figure below is an illustration of version 1.5 of LOAC, which has been improved to produce version 2, in service since the beginning of 2025.

. **Figure 1 :** Image of LOAC version 1.5 on the left and version 2 on the right

2.1.2. Principle of LOAC instrument measurements

The LOAC (Light Optical Aerosol Counter) instrument is a particle counter that provides aerosol concentration data at ground level or during flight using a weather balloon to measure concentration profiles along the atmospheric column from the troposphere to the stratosphere. Measurements are taken in 19 size ranges between 0.2 and 50 micrometers and in different atmospheric layers up to an altitude of 34 km, depending on atmospheric conditions. In addition, an M10 or M20 weather probe equipped with humidity and temperature sensors and a GPS (position detection) is attached to the instrument during flights to provide information on the profile of the thermodynamic parameters of the atmosphere. LOAC measurements are based on the principle of particle scattering in a light beam emitted by photodiodes, with the scattered intensity proportional to the size and refractive index of the particle. In addition, observations are made at two scattering angles (12° and 60°), providing information on the nature of the particles and enabling their chemical type (rough chemical nature). The entire system is powered by rechargeable batteries with a minimum autonomy of three hours, and the data is either transmitted by telemetry or recorded directly to a storage memory using a data logger. It should be noted that the LOAC instrument weighs 250 g and has a nominal electrical power of 3 watts. The data can also be viewed on a computer connected to the ground via a receiving station. In fact, the LOAC instrument incorporates an Internet of Things system designed using a specially adapted card that allows automatic access to data during measurements via a transmission signal. All of the devices are housed in a box-shaped gondola, with the telemetry and batteries weighing 1 kg. The pod is connected to a weather balloon containing a gas (helium or hydrogen) whose quantity is proportional to the mass of the equipment to be transported, including the tether and the parachute used to regulate the descent of the instruments when the balloon bursts. Note that the parachute is attached between the balloon and the basket, allowing it to open if the balloon bursts and then subjecting it to the effect of the air mass. In addition, the balloon's trajectory is tracked directly online during the flight on the weather website (https://sondehub.org/) using M10 or M20 weather sensors until it falls, allowing the measuring equipment to be recovered. However, this trajectory is predicted (https://predict.sondehub.org/) on the eve of the campaign and then sent to the local military agency and civil aviation authority in order to obtain approval from the authorities depending on the area being flown over. It should be noted that LOAC v1.5, which was replaced in 2025 by version 2, which was completely revised in terms of optics, electronics, and processing software, may have difficulty operating optimally at high temperatures.

2.1.3. Methodological approach for balloon flight measurement

Before the start of any LOAC balloon flight, meticulous work is carried out to ensure optimal conditions for safe and successful measurement:

- **Instrument control**

This first step involves cleaning the particle sampling pump chamber, followed by a check of the pod's condition to ensure there is no damage. The batteries in the M20 weather probe are replaced and the probe is tested for temperature, humidity, and pressure measurements, as well as GPS coordinates for the system's trajectory during flight. In addition, the LOAC battery is recharged and the instrument is tested in flight configuration with data transmission via radio communication through a receiving station installed on the roof of the LPC2E.

- **Tare calculation**

For all balloon flights, the tare method is used to determine the amount of gas needed to inflate the balloon. Thus, the mass of the gas (hydrogen or helium) is the sum of the masses of the LOAC instrument and its accessories, including the M20 weather probe, GPS tracker, parachute, tether, and gondola, in addition to the free lift force. For a typical LOAC flight, the tare weight is estimated at approximately 2400g.

- **Administrative aspects**

This includes checking the balloon's projected trajectory on the eve of the planned flight and the weather conditions. Next, a flight authorization request is sent to the military air base to obtain approval and support from the army responsible for airspace control. In addition, a flight plan is drawn up and a trajectory simulation is performed just before the balloon is released to ensure that it still corresponds to the initial forecasts. A final call is made to the air base approximately 30 minutes before the balloon is released in order to contact the pilot and warn him of a balloon release in the vicinity of the control zone.

- **The flight chain**

All elements constituting the flight are configured according to the defined diagram: the balloon – the parachute – the gondola containing LOAC and its accessories. For LOAC flights, BLD (Ballon Léger Dilatable) balloons are used, and the maximum weight under a BLD is 3 kg plus the lift force, which is approximately 1.7 kg but estimated at 1 kg. For LOAC flights, the mass of the BLD balloon, depending on weather conditions, is 1000 g or 1200 g with a 4- or 5-foot parachute. The mass of the gondola containing the LOAC and its equipment is 1100 g. Figure 2 below illustrates the flight chain, with the balloons inflated with hydrogen gas in accordance with the tare weight on the left and the LOAC instruments contained in the gondolas and the metrological probes on the right. A parachute is attached to the end of each balloon, which will be connected to the gondola by a wire.

Figure 2 : Illustrative images of preparations for a balloon flight at the Orleans site

2.2. EarthCare (Cloud, Aerosol and Radiation Explorer)

EarthCare is currently the largest satellite for observing the Earth's atmosphere, launched by the European Space Agency (ESA) in collaboration with JAXA (Japan Aerospace Exploration Agency) on May 28, 2024. Its role is to contribute to a better understanding of the exact role of aerosols and clouds in the climate system through their interactions with incident solar and infrared radiation. Placed in an orbit at an altitude of approximately 390 km, EarthCare carries four instruments, each equipped with a different observation technique, enabling it to view the entire Earth and provide information on the atmosphere and its components, particularly aerosols and clouds. These include the atmospheric lidar (ATLID), which provides vertical profiles of aerosols and fine clouds at a wavelength of 355 nm with a spatial resolution of approximately 103 m to 500 m. It has a high spectral resolution receiver and a depolarization channel. This is also the case for the broadband radiometer (BBR), which measures radiance (emitted or reflected radiation) and fluxes at the surface of the atmosphere. In addition, EarthCare carries a cloud profiling radar (CPR) that measures the vertical profiles of clouds and observes the vertical velocities of cloud particles using the Doppler effect, as well as a multispectral imager (MSI) that provides cross-sectional information on clouds and aerosols in various channels, including the visible to infrared spectrum. The following figure shows the instruments used to summarize the EarthCare satellite's missions.

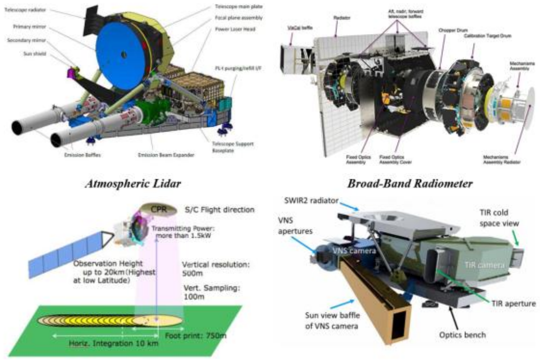

Figure 3 : EarthCare satellite instruments

2. 3. Community Earth System Model (CESM)

CESM (Community Earth System Model) is a fully coupled global model of the Earth's climate system developed by NCAR (National Center for Atmospheric Research) in the United States in collaboration with researchers from the scientific community [13]. CESM provides state-of-the-art simulations that provide information on the past, present, and future states of the Earth system [14]. It allows us to explore the complex interactions between the different components of the climate system and to assess the impact of human activities and natural processes on the climate. CESM2 is version 2 of the coupled model, which integrates several sub-models representing different parts of the Earth's climate system. To this end, we distinguish between the CAM6 (Community Atmosphere Model version 6) atmospheric model, the POP2 (Parallel Ocean Program) ocean model, the CLM5 (Community Land Model) land model, the CICE5 model for studying sea ice, and the CISM2 (Community Ice Sheet Model) model adapted to the study of ice on land [14]. The components of the CESM2 model and the various couplings are illustrated in the figure below and clearly described by several authors [14], [15]. In addition, these different variable prediction models are connected to a common Earth modeling infrastructure that contains the coupling system, scripting support, data models, and libraries needed to run CESM2 as a single executable. The CAM6 atmospheric model is dedicated to the study of aerosols, clouds, atmospheric chemistry, and atmospheric dynamics based on climate variables such as temperature, wind, humidity, precipitation, and radiation. It provides simulations for four aerosol modes, namely the Aiken mode, accumulation mode, coarse mode, and primary carbon mode [16], [17]. This makes it possible to track the optical and microphysical behavior of each aerosol population, in particular through the vertical profile of aerosol optical depth (AOD), extinction, and particle volume concentration according to mode from the troposphere to the stratosphere.

2. 4. MODIS (MODerate Resolution Imaging Spectro-radiometer)

MODIS is a sensor carried by the TERRA satellite since December 1999 and by Aqua since April 2002. TERRA scans the Earth's surface from north to south around the equator in the morning at around 10:30 a.m., while Aqua passes in the evening at around 1:30 p.m. on a south-north orbit of the equator [18]. MODIS has 36 spectral bands that enable it to provide measurements on the atmosphere, land, and ocean, seven of which are intended for the study of aerosols (466, 553, 644, 855, 1243, 1632, and 2119 nm). In addition, it uses different algorithms to invert aerosol properties at the Earth [19] and ocean [20] levels, where measurements are taken with a spatial resolution ranging from 1 to 250 km and a temporal resolution ranging from 1 to 2 days. For our study, we use MODIS-Terra Deep-Blue inversions at 550 nm, available on NASA's Giovanni website (https://giovanni.gsfc.nasa.gov/giovanni/). The Deep Blue algorithm takes into account cloud masks, the aerosol model, and the reflection of shiny surfaces [18], [21]. This eliminates contamination due to the reflection of shiny surfaces and improves Level 2 observations of surfaces such as the Sahara Desert, arid, semi-arid, and urban regions where reflectivity is very high [22].

2. 5. Modern-Era Retrospective Analysis for Research and Applications (MERRA)

In this work, we use wind data at 10 m altitude derived from MERRA model rea- nalysis. Indeed, these reanalysis are based on satellite observations from NASA and are available from 1979 to the present days. The model was initiated by NASA and is especially suitable for climatic analysis whose data are available continuously and then in the long-term on NASA’s Giovanni site.

3- Results and discussion

3.1. Processing and analysis of data from LOAC instrument measurements

3.1.1. Representation of aerosol vertical profiles

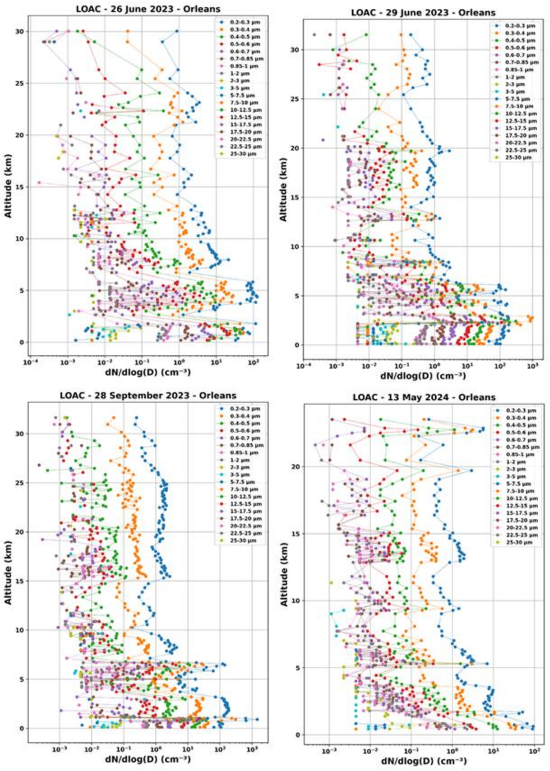

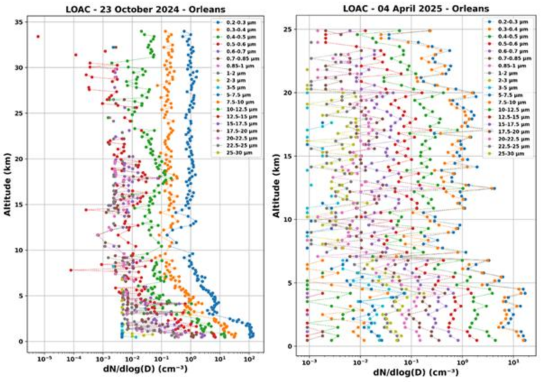

Figure 4 : Aerosol profiles at the Orleans site for different measurement campaigns

The various figures above illustrate the aerosol profiles represented based on measurements taken by the LOAC instrument. This is historical data obtained from measurement campaigns carried out between 2023 and 2025. It shows the variability of each particle size range across the different atmospheric layers, from the troposphere to the stratosphere. High volume concentrations are observed in the lower tropospheric layers and mainly concern fine particles probably linked to urban pollution and the transport of particles generated by biomass combustion, particularly forest fires. However, the volume density values of large particles with a radius greater than 1 µm may be due to ice crystals attributed to clouds.

3.1.2. Evaluation of aerosol size distribution

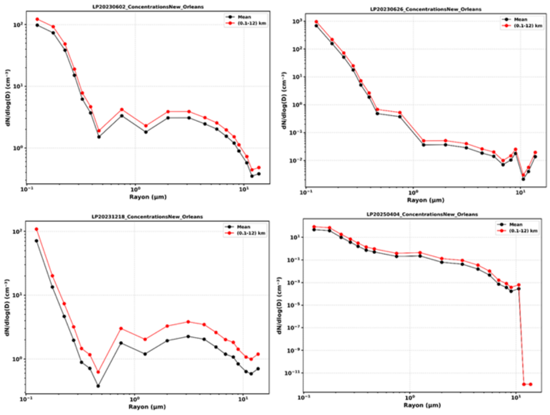

Figure 5 : Volume size distribution of aerosols at the Orleans site

The particle size distribution calculated from LOAC measurements refers to the number distribution, which clearly shows the evolution of the size class of aerosol particles in the atmospheric layer. The black curve corresponds to the average number distribution throughout the atmospheric layer measured from the troposphere to the stratosphere during the balloon flight, while the red curve represents the average number distribution estimated in the troposphere. The volume number distribution above the average confirms the hypothesis of high particle concentration in the lower atmosphere. In addition, from all the measurements, we note a dominance of the aerosol population by fine mode particles (r ≤ 1µm) given their greater number. In addition, the various figures highlight an aerosol population characterized by an Aiken mode (r ≤ 0.5 µm), an accumulation mode (0.5 µm ≤ r ≤ 1µm), and a coarse mode associated with particles of size r ≥ 1µm.

3.1.3. Assessment of PM_1, $PM_{2.5}$, and PM_{10}

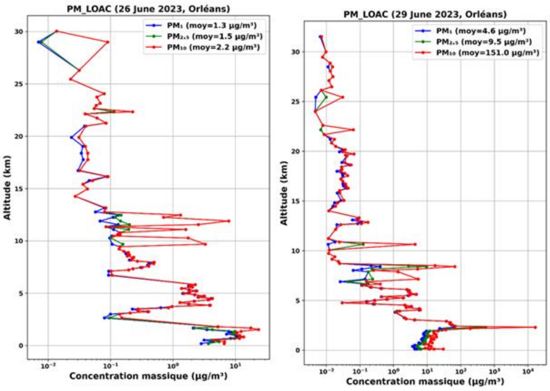

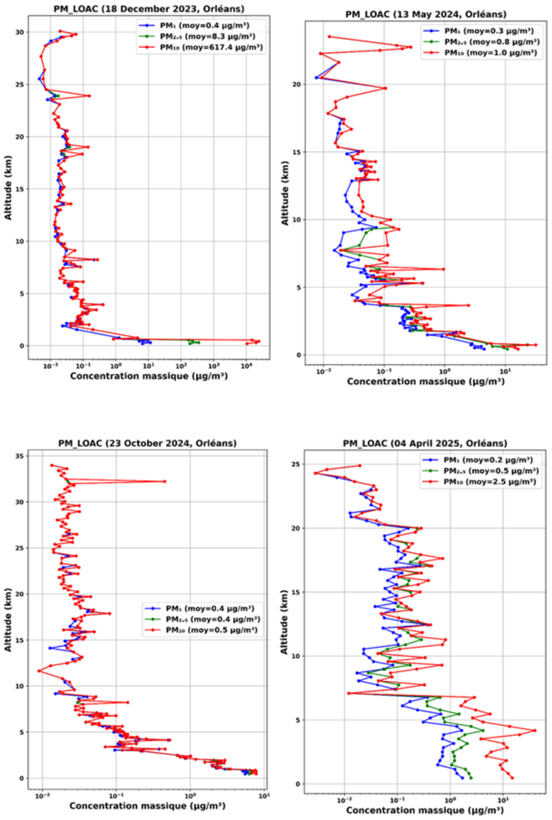

Figure 6 : Representation of PM_1, $PM_{2.5}$, and PM_{10} fine particle profiles at the Orleans site

The vertical profiles of PM_1, $PM_{2.5}$, and PM_{10} were calculated from the number concentrations obtained from the LOAC instrument, converted to mass using the method described in [23], assuming an average particle density of 1.5 g/cm³ corresponding to mineral or urban particles [24]. The indices (PM_1, $PM_{2.5}$, PM_{10}) represent the total mass fraction of particles with a diameter below a threshold. PM_1 includes fine particles smaller than 1 µm (r ≤ 1 µm) and $PM_{2.5}$ includes those smaller than 2.5 µm (r ≤ 2.5 µm), composed of Aiken and accumulation particles, while PM_{10} represents particles smaller than 10 µm (r ≤ 10 µm), including some large particles. This representation clearly shows the evolution of each size class at varying concentrations depending on different altitude levels. However, high concentrations are more noticeable in the lower and middle atmospheric layers located in the troposphere below 10 km altitude. This is consistent with the health impact of aerosols, whose toxicity depends on particle size, especially the smallest particles, such as PM_1, which can penetrate the respiratory system down to the alveoli and easily pass into the bloodstream. As a result, every year 4 to 7 million people die prematurely and hundreds of millions more suffer from diseases caused by air pollution, which is responsible for enormous suffering [25]. These figures also illustrate the average concentration of PM_1, $PM_{2.5}$, and PM_{10} for each day of measurement at varying proportions, which are certainly justified by atmospheric dynamics and anthropogenic pollution.

3.1.4. Calculation of aerosol extinction

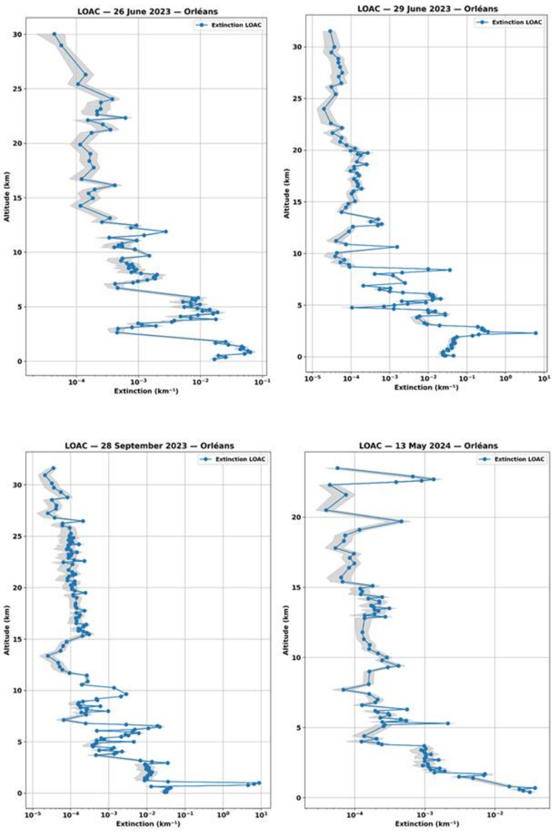

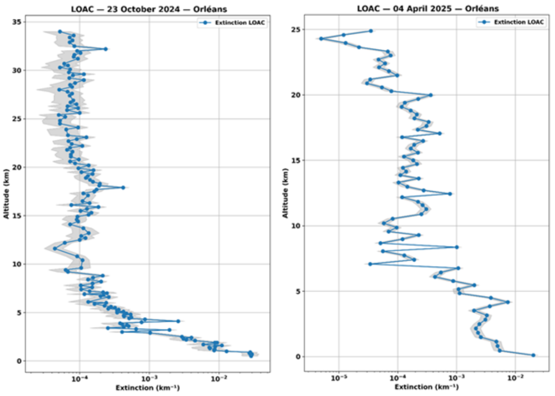

Figure 7 : Profile of aerosol extinction at the Orleans site between 2023 and 2025

The extinction coefficient is an optical property that quantifies the impact of aerosols on the radiative balance of the climate system. The figure above shows the extinction of solar radiation through the atmospheric layer due to the direct effect of aerosols (absorption and scattering). It illustrates the high variability of extinction, with notable peaks depending on the day. These peaks are synonymous with an aerosol layer characterized by a high concentration, which is distinguished by a strong attenuation of the incident solar flux. However, extinction values greater than unity calculated at the surface of the troposphere may be due to the albedo of cloud particles, given the high humidity that can lead to ice crystals following condensation of water vapor and cloud cover. In addition, the extinction peaks observed in the middle troposphere at altitudes above 5 km and in the stratosphere above 10 km demonstrate the ability of aerosols to modify the chemical composition and thermodynamic parameters (temperature, humidity, etc.) of the atmosphere. They can also influence the microphysical properties of clouds and their precipitation capacity.

3.1.5. Calculation of Aerosol Optical Depth

Based on the extinction obtained using Mie scattering theory, we were able to determine the average daily AOD, which is an integration of the extinction coefficient according to the atmospheric layer, the values of which are summarized in Table 1 below. In fact, to calculate this optical parameter for aerosols, we limited ourselves to particles contained in the troposphere, estimated at altitudes between approximately 0 and 12 km. This exercise enabled us to convert the aerosol concentrations measured by the particle counter (LOAC) into an optical property (AOD). However, for a study applied to a given area, the height of the atmospheric layer could be adjusted and adapted according to scientific debate.

Table 1 : Aerosol Optical Depth at the Orleans site

Date	27/04/2023	26/05/2023	02/06/2023	16/06/2023	26/06/2023
AOD	0.0210 ± 0.0013	0.0511 ± 0.0025	0.6320 ± 0.0065	0.0450 ± 0.0021	0.0908 ± 0.0045

Date	29/06/2023	28/09/2023	28/11/2023	18/12/2023	13/05/2024
AOD	1.1098 ± 0.0284	2.3589 ± 0.0254	0.0120 ± 0.0013	2.1180 ± 0.0170	0.0191 ± 0.0013

Date	23/10/2024	04/04/2025
AOD	0.0257 ± 0.0020	0.0194 ± 0.0010

AOD is an indicator of atmospheric aerosol load and provides information on visibility and air quality. However, the state of the atmosphere defined by AOD depends on the location and nature of the suspended particles. To this end, studies carried out in the Sahel region of West Africa have identified four types of days based on AOD values and the Angström coefficient [26], [27]. Thus, when the aerosol optical depth (AOD) is less than or equal to 0.15, $(\mathrm{AOD} \leq 0.15)$ the day is considered clear regardless of the Angström coefficient value. For AOD values between 0.2 and 0.5 $(0.2 \leq \mathrm{AOD} \leq 0.5)$ associated with Angström coefficient values below 0.4 $(\alpha_{440\text{-}870} < 0.4)$, the day is considered standard. When AOD values are above 0.15 $(\mathrm{AOD} > 0.15)$ and correspond to Angström coefficient values below 0.4 $(\alpha_{440\text{-}870} < 0.4)$, the day is considered dusty. In addition, mixed days are defined and correspond to AOD values greater than 0.15 $(\mathrm{AOD} > 0.15)$ and Angström coefficient values greater than 0.4 $(\alpha_{440\text{-}870} > 0.4)$.

3.1.6. Comparison of LOAC measurements and ATLID lidar from the EarthCare satellite

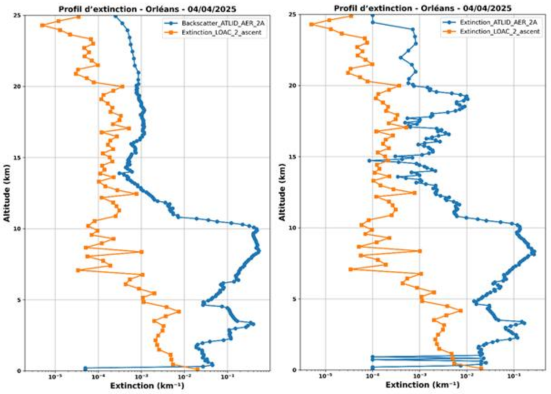

Figure 8 : Extinction profile between LOAC and ATLID AER 2A

This representation is an exercise based on mastering the processing of ATLID lidar measurements aboard the EarthCare satellite, launched into orbit on May 28, 2024, by the European Space Agency (ESA) in collaboration with JAXA (Japan Aerospace Exploration Agency). The LPC2E laboratory is participating in the ATLID lidar measurement validation program through the LOAC instrument, and flights are being initiated at several sites, including Orleans, depending on the day and the satellite's trajectory. This is a new approach for us in the optical and microphysical characterization of aerosols, which will be applied in Burkina Faso and West Africa in general. This validation allows the inversion algorithms to be adjusted or corrected to take into account the actual aerosol population, which depends on the area surveyed by the lidar signal. It should be noted that this aerosol population varies greatly due to multiple sources, particularly in the Sahel, which is experiencing strong population growth [28]. However, caution is advised when using EarthCare data, which is still undergoing validation, even though the initial results are conclusive [29].

3.2. Modeling aerosols in West Africa using the CESM2 model

3.2.1. Seasonal analysis of aerosols using the CESM model

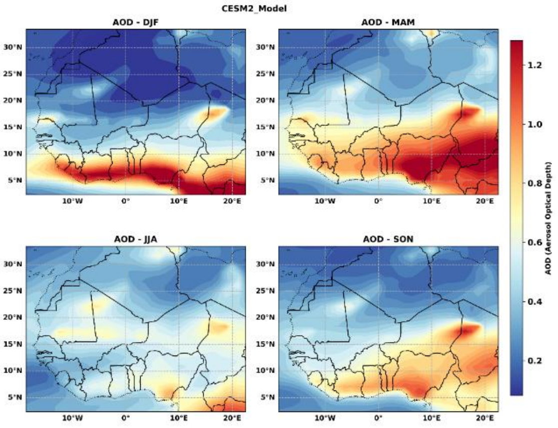

Figure 9 : Seasonal cycle of total aerosol AOD from the CESM2 model

The figure above shows the seasonality of aerosols in West Africa using simulations from the CESM global climate model developed by the LPC2E laboratory between 2013 and 2018. It shows the interannual spatial variability of aerosols, with maxima illustrated by high AOD values observed during the winter (DJF), spring (MAM), summer (JJA), and fall (SON) periods. The notable points or spots highlight potential emission sources located on either side of the sub-region and are active according to the seasons defined by the periods.

Thus, biomass combustion sources, which are more active in winter, are mainly observed in the Gulf of Guinea in the south. This modeling reveals a period of high aerosol emissions during the spring, marked by a mixture of combustion particles and desert dust coming from the northeast. This aerosol climatology is governed by regional atmospheric dynamics defined by monsoon and harmattan flows.

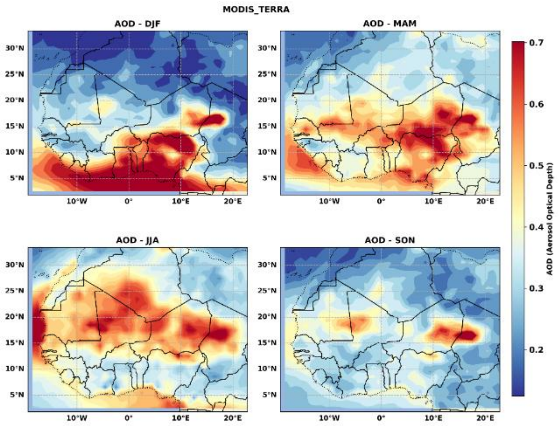

Figure 10 : Seasonal cycle of total aerosol AOD from the MODIS sensor

In comparison with satellite observations from the MODIS sensor (Figure 10) aboard NASA's TERRA observation satellite, we note a simulation of aerosol seasonality in the West African region as a whole. However, the AOD values are overestimated by the CESM2 model, which calculates maxima between 1 and 1.2, whereas MODIS indicates values around 0.7 according to the legend. Like MODIS, a specific analysis focusing solely on mineral dust, illustrated in Figure 11 below, reveals the seasonality of these particles, which are present throughout the year and evolve according to the seasons defined by the dynamics of the monsoon and Harmattan winds. Thus, dust is more prevalent in winter and spring, in line with the northeast Harmattan winds, which are responsible for transporting and distributing these mineral particles throughout West Africa as far as the Gulf of Guinea. The main sources of dust emissions include the Bodélé Depression in eastern Niger and Chad, southern Algeria and northwestern Mali, and the border area between Mali and Mauritania. These sources are consistent with previous studies that identified dust sources in the semi-arid and arid zones of West Africa in the Sahel and Sahara [30], [31].

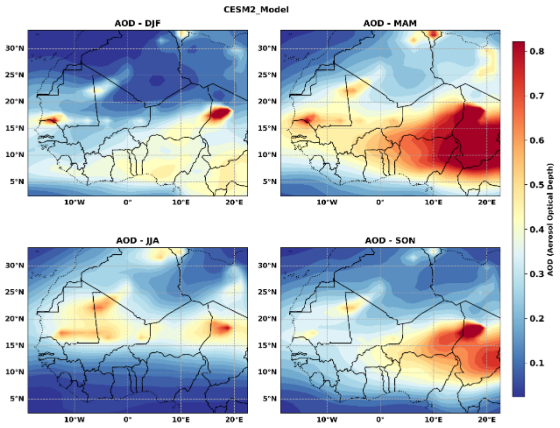

Figure 11 : Seasonal cycle of mineral dust AOD from the CESM2 model

During the period of monsoon dominance in summer (JJA), dust is more intense in the northern Sahara due to the arrival of the intertropical convergence zone, which is located at its most stable position around 10°N [32]. The presence of this humid convection over the continent explains the heavy rains in summer in the Sahel and the Gulf of Guinea, hence the absence of dust during this period below 15°N according to the CESM2 model (Figure 11). However, MODIS clearly shows the impact of convective systems in summer, which are accompanied by very violent air currents and are responsible for significant local dust mobilization, in addition to the long-distance transport of fine desert particles at medium and high altitudes in the Saharan air layer. The autumn period is a transition marked by the retreat of the monsoon southwards below 5°N latitude [32], [33]. During this time, the harmattan remains weak but begins to make itself felt with the arrival of dust carried by north-easterly winds, especially on the eastern side with the activation of the Bodélé Depression.

3.2.2. Validation tests and local study of aerosol emissions in West Africa

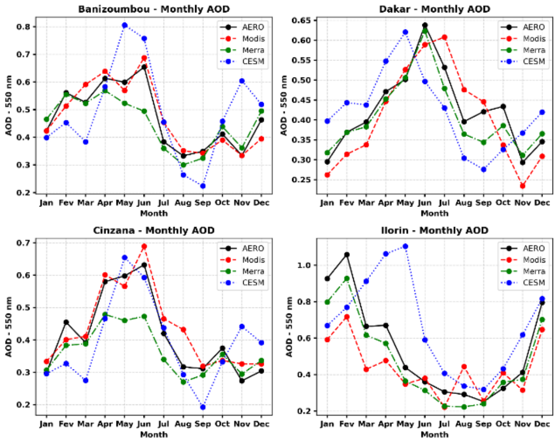

Figure 12 : Annual cycle of AOD at 550 nm at sites located in West Africa

The figure above shows the annual cycles of AOD at 550 nm based on several approaches using in situ measurements from the AERONET network, satellite observations from the MODIS sensor, and simulations from the MERRA and CESM2 models. The aim is to demonstrate the accuracy of the CESM2 model in studying aerosols at the local level in West Africa. To do this, we listed sites located in the latitude band between 12°N and 18°N, including Banizoumbou (13.541˚N, 02.665˚E) located 50 km from Niamey in Niger, Cinzana (13.278˚N, 05.934˚W) in Mali, Dakar (14.394˚N, 16.959˚W) in Senegal, and Ilorin (08.5˚N, 4.7˚E) in Nigeria. In addition, these sites are chosen based on the availability of AERONET data covering the period from 2013 to 2018 in accordance with the CESM2 model outputs. Compared to in situ measurements and satellite observations, the CESM2 model broadly reproduces the AOD peak, albeit with a shift in the peak corresponding to the aerosol maxima at the various sites. As for the MERRA model, it simulates aerosols better locally, especially at the Dakar and Ilorin sites, but significantly underestimates them in the case of Banizoumbou and Cinzana. In the Sahel, at Banizoumbou, Cinzana, and Dakar, the AOD peak is observed in June, consistent with the turbulence of convective systems, while the CESM2 model shows it in May for all sites. This peak is inconsistent with the period of high particulate emissions in winter in February at the Ilorin site located in the Gulf of Guinea.

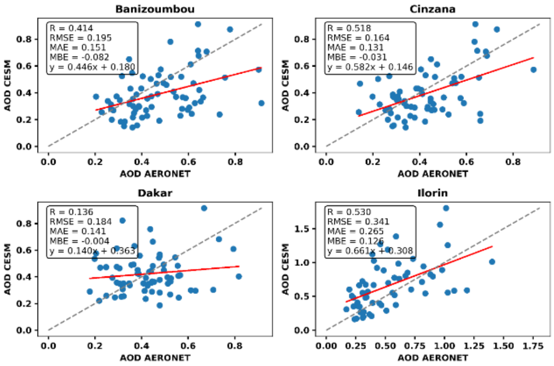

Figure 13 : Representation of linear regression and calculation of statistical indices

Furthermore, a representation of the linear regression lines (Figure 13) shows an average correlation between the CESM2 and AERONET models at the Cinzana and Ilorin sites, with estimated coefficient values of around 0.50, compared to 0.414 at Banizoumbou and 0.136 at the Dakar site. In addition, we use statistical indicators that define the accuracy of the model in relation to in situ measurements. These include the root mean square error (RMSE), which illustrates the variation in simulated AOD relative to ground measurements, and the mean absolute error (MAE). The smaller the RMSE and MAE values, the more accurate the model. We also calculate the mean bias error (MBE), which gives an indication of the average deviation of the CESM2 model's AOD from AERONET measurements. A positive MBE value indicates an overestimation, while a negative value indicates an underestimation [34]. Thus, the MBE values clearly highlight an underestimation of in situ measurements by the CESM2 model at the Banizoumbou, Cinzana, and Dakar sites, and confirm the overestimation of AOD at Ilorin. However, the performance indicators show that the model is poorly suited to locally modeling the aerosol cycle at sites in West Africa. In agreement with Yusuf et al., 2023, this could be justified by a divergence between the aerosol model integrated into the CESM2 simulation algorithms and the actual aerosol population observed at the study sites [35]. In addition, the aerosol population in West Africa varies greatly and is not homogeneous, given the multiple sources of natural and anthropogenic origin. To this end, local sources may be poorly estimated by the simulation model, leading to very low correlation coefficients, particularly at the Dakar and Banizoumbou sites.

4- Conclusion

The research stay at the LPC2E laboratory was a time of learning, discovery, and sharing experiences for us, both scientifically and culturally. In line with the research project based on new techniques for the optical and microphysical characterization of aerosols available at LPC2E, we first took stock of all the necessary equipment. This enabled us to understand the operating and measurement principles of the LOAC instrument, as well as the methodological approach to be adopted for conducting a balloon flight. Next, we analyzed the LOAC data using Python programming, which consisted of converting this data into optical and microphysical properties that define the impact of aerosols on health, climate, and the environment. Finally, we analyzed simulations from the CESM2 global model and satellite observations from the MODIS sensor, the ATLID lidar, and the MERRA model outputs. This made it possible to represent the aerosol climatology in West Africa based on seasonal and annual cycles of aerosol optical depth (AOD) at a wavelength of 550 nm. This was an exercise that we intend to continue and apply in Burkina Faso to study air quality, which is severely degraded due to the frequency of dust events and local pollution, especially during winter and spring. It should also be noted that this report is a brief summary and partial presentation of the results obtained during the three months spent at LPC2E.

5- Perspectives of future collaborations with the host laboratory

The research stay was an opportunity for Joseph KI-ZERBO University to establish collaboration with the CNRS's LPC2E in Orléans, particularly in the field of research for student training and supervision. In addition, there are plans to acquire optical instruments, notably LOAC, on the basis of a project to enable Burkina Faso to conduct its own measurement campaigns for better monitoring of air quality and assessment of the climate and health impact of aerosols. To this end, the LPC2E could assist with equipment maintenance and staff training in the use of the instruments and the processing of measurement data. Burkina Faso will also be able to benefit from the LPC2E's CESM2 global chemistry transport model simulations for optical and microphysical modeling of aerosols in West Africa.

6- Articles published in the framework of the fellowship

Not applicable

7- Acknowledgements

We would like to express our warmest thanks to the LPC2E at the CNRS in Orléans for hosting us and supporting our research project.

We would also like to thank the entire LE STUDIUM team for the research stay, which enabled us to collaborate and exchange scientific ideas with other international researchers and experts.

8- References

[1] J. L. Rajot, A. A. Touré, K. Desboeufs, P. Formenti, B. Marticorena, and M. Sow, "Le cycle des aérosols terrigènes au Sahel : ce qu'AMMA nous a appris," *La Météorologie*, vol. 8, no. Special-AMMA, p. 33, 2012, doi: 10.4267/2042/48130.

[2] B. Nébon, M. S. Dramé, K. Bruno, K. P. Florent, S. M. Sall, and D. Joseph, "Optical and microphysical analysis of aerosols in Sahelian Zone : Case of the Ouagadougou City in Burkina Faso," *Elixir International Journal*, vol. 119, pp. 50975–50982, 2018.

[3] C. Liousse and C. Galy-Lacaux, "La Météorologie-n° 71-novembre 2010 Environnement Pollution urbaine en Afrique de l'Ouest," pp. 45–49, 2010.

[4] J. M. Haywood *et al.*, "Overview of the Dust and Biomass-burning Experiment and African Monsoon Multidisciplinary Analysis Special Observing Period-0," *J Geophys Res*, vol. 113, no. October, pp. 1–20, 2008, doi: 10.1029/2008JD010077.

[5] C. Liousse *et al.*, "Updated African biomass burning emission inventories in the framework of the AMMA-IDAF program, with an evaluation of combustion aerosols," *Atmos Chem Phys*, vol. 10, no. 19, pp. 9631–9646, 2010, doi: 10.5194/acp-10-9631-2010.

[6] G. Myhre *et al.*, "Modeling the radiative impact of mineral dust during the Saharan Dust Experiment (SHADE) campaign," *J Geophys Res*, vol. 108, no. D18, p. 8579, 2003, doi: 10.1029/2002JD002566.

[7] B. Zhang, "The Effect of Aerosols to Climate Change and Society," *Journal of Geoscience and Environment Protection*, vol. 08, no. 08, pp. 55–78, 2020, doi: 10.4236/gep.2020.88006.

[8] K. Ramgolam *et al.*, "Size-partitioning of an urban aerosol to identify particle determinants involved in the proinflammatory response induced in airway epithelial cells," *BioMed Central*, vol. 6, pp. 1–12, 2009, doi: 10.1186/1743-8977-6-10.

[9] B. Korgo *et al.*, "Diurnal Variability of the Radiative Impact of Atmospheric Aerosols in Ouagadougou, Burkina Faso : A Seasonal Approach," *J Environ Prot (Irvine, Calif)*, vol. 11, no. 12, pp. 1089–1102, 2020, doi: 10.4236/jep.2020.1112069.

[10] B. Korgo *et al.*, "The Radiative Forcing of Aerosols in a West Africa Sahelian Urban City : Case Study of Ouagadougou," *Atmospheric and Climate Sciences*, vol. 11, no. 01, pp. 73–85, 2021, doi: 10.4236/acs.2021.111005.

[11] B. Nébon *et al.*, "Study of Aerosol Impact on the Solar Potential Available in Burkina Faso, West Africa," *International Journal of Environment and Climate Change*, vol. 9, no. 5, pp. 297–310, 2019, doi: 10.9734/ijecc/2019/v9i530116.

[12] C. Chou *et al.*, "Size distribution, shape, and composition of mineral dust aerosols collected during the African Monsoon Multidisciplinary Analysis Special Observation Period 0 : Dust and Biomass-Burning Experiment field campaign in Niger, January 2006," *Geophysical Research*, vol. 113, no.

January 2006, pp. 1–17, 2008, doi: 10.1029/2008JD009897.

[13] I. Davis and B. Medeiros, “Assessing CESM2 Clouds and Their Response to Climate Change Using Cloud Regimes,” *J Clim*, vol. 37, no. 10, pp. 2965–2985, 2024, doi: 10.1175/JCLI-D-23-0337.1.

[14] G. Danabasoglu *et al.*, “The Community Earth System Model Version 2 (CESM2),” *J Adv Model Earth Syst*, vol. 12, no. 2, pp. 1–35, 2020, doi: 10.1029/2019MS001916.

[15] A. N. Sommers *et al.*, “Retreat and Regrowth of the Greenland Ice Sheet During the Last Interglacial as Simulated by the CESM2-CISM2 Coupled Climate–Ice Sheet Model,” *Paleoceanogr Paleoclimatol*, vol. 36, no. 12, pp. 1–19, 2021, doi: 10.1029/2021PA004272.

[16] S. Tilmes *et al.*, “Description and performance of a sectional aerosol microphysical model in the Community Earth System Model (CESM2),” *Geosci Model Dev*, vol. 16, no. 21, pp. 6087–6125, 2023, doi: 10.5194/gmd-16-6087-2023.

[17] D. Watson-Parris *et al.*, “Surface temperature effects of recent reductions in shipping SO2 emissions are within internal variability,” *Atmos Chem Phys*, vol. 25, no. 8, pp. 4443–4454, 2025, doi: 10.5194/acp-25-4443-2025.

[18] R. C. Levy, L. A. Remer, S. Mattoo, E. F. Vermote, and Y. J. Kaufman, “Second-generation operational algorithm : Retrieval of aerosol properties over land from inversion of Moderate Resolution Imaging Spectroradiometer spectral reflectance,” *J Geophys Res*, vol. 112, pp. 1–21, 2007, doi: 10.1029/2006JD007811.

[19] Y. J. Kaufman, D. Tanr, L. A. Remer, E. F. Vermote, and A. Chu, “Operational remote sensing of tropospheric aerosol over land from EOS moderate resolution imaging spectroradiometer,” *J Geophys Res*, vol. 102, no. 96, pp. 51–67, 1997, doi: 10.1029/96JD03988.

[20] D. Tanré, Y. J. Kaufman, M. Herman, and S. Mattoo, “Remote sensing of aerosol properties over oceans using the MODIS / EOS spectral radiances,” *J Geophys Res*, vol. 102, no. 3, pp. 16,971-16,988, 1997.

[21] L. A. Remer *et al.*, “The MODIS Aerosol Algorithm, Products, and Validation,” *American Meteorological Society*, vol. 62, pp. 947–973, 2005.

[22] N. C. Hsu, S. Tsay, M. D. King, S. Member, and J. R. Herman, “Aerosol Properties Over Bright-Reflecting Source Regions,” *IEEE Transactions on Geoscience and Remote Sensing*, vol. 42, no. 3, pp. 557–569, 2004.

[23] J. B. Renard *et al.*, “LOAC : A small aerosol optical counter/sizer for ground-based and balloon measurements of the size distribution and nature of atmospheric particles-Part 2 : First results from balloon and unmanned aerial vehicle flights,” *Atmos Meas Tech*, vol. 9, no. 8, pp. 3673–3686, 2016, doi: 10.5194/amt-9-3673-2016.

[24] J. P. Putaud *et al.*, “A European aerosol phenomenology – 2 : Chemical characteristics of particulate matter at kerbside, urban, rural and background sites in Europe,” *Atmos Environ*, vol. 38, no. 16, pp. 2579–2595, 2004, doi: 10.1016/j.atmosenv.2004.01.041.

[25] M. Z. Jacobson *et al.*, “100% Clean and Renewable Wind, Water, and Sunlight All-Sector Energy Roadmaps for 139 Countries of the World,” *Joule*, vol. 1, no. 1, pp. 108–121, 2017, doi: 10.1016/j.joule.2017.07.005.

[26] M. S. Drame *et al.*, “On the Importance of Aerosol Composition for Estimating Incoming Solar Radiation : Focus on the Western African Stations of Dakar and Niamey during the Dry Season,” *Atmosphere (Basel)*, vol. 6, pp. 1608–1632, 2015, doi: 10.3390/atmos6111608.

[27] N. Bado, E. Korsaga, B. Dianda, M. S. Dramé, B. Korgo, and F. P. Kieno, “Impact of typical days on the optical and microphysical parameters of aerosols in urban zone of Burkina Faso, West Africa,” *Asian Journal of Atmospheric Environment*, vol. 19, no. 1, 2025, doi: 10.1007/s44273-025-00055-2.

[28] J. L. Rajot, A. A. Touré, K. Desboeufs, P. Formenti, B. Marticorena, and M. Sow, “Le

cycle des aérosols terrigènes au Sahel : ce qu'AMMA nous a appris," *La Météorologie*, vol. 8, no. Special-AMMA, p. 33, 2012, doi: 10.4267/2042/48130.

[29] L. Pfitzenmaier, P. Kollias, N. Risse, I. Schirmacher, B. Puigdomenech Treserras, and K. Lamer, "Orbital-Radar v1.0.0: a tool to transform suborbital radar observations to synthetic EarthCARE cloud radar data," *Geosci Model Dev*, vol. 18, no. 1, pp. 101–115, 2025, doi: 10.5194/gmd-18-101-2025.

[30] S. Engelstaedter and R. Washington, "Atmospheric controls on the annual cycle of North African dust," vol. 112, 2007, doi: 10.1029/2006JD007195.

[31] S. Engelstaedter and R. Washington, "Temporal controls on global dust emissions : The role of surface gustiness," *Geophys Res Lett*, vol. 34, pp. 1–5, 2007, doi: 10.1029/2007GL029971.

[32] A. Kouassi *et al.*, "Étude du climat Ouest-Africain à l'aide du modèle atmosphérique régional M.A.R.," *Climatologie*, vol. 7, pp. 39–55, 2010, doi: 10.4267/climatologie.445.

[33] B. Sultan and S. Janicot, "Abrupt shift of the ITC Z over West Africa and intra-seasonal variability," *Geophys Res Lett*, vol. 27, no. 20, pp. 3353–3356, 2000.

[34] N. Bado, M. Ladifata, Y. W. Charles, T. Karim, and F. P. Kieno, "Seasonal Analysis of Aerosol Frequency and Assessment of the Radiative Impact of a Dust Episode in Burkina Faso, West Africa," *Physical Science International Journal*, vol. 29, no. 3, pp. 50–61, 2025, doi: 10.9734/psij/2025/v29i3883.

[35] N. Yusuf and R. S. Said, "Spatial distribution of aerosols burden and evaluation of changes in aerosol optical depth using multi-approach observations in tropical region," *Heliyon*, vol. 9, no. 8, p. e18815, 2023, doi : 10.1016/j.heliyon. 2023.e18815.